RSC Advances

PAPER

View Article Online
View Journal | View Issue

Open Access Article. Published on 08 July 2024. Downloaded on 11/7/2025 2:05:18 AM.
This article is licensed under a Creative Commons Attribution-NonCommercial 3.0 Unported Licence.

Check for updates

Cite this: *RSC Adv.*, 2024, **14**, 21432

Synthesis and mutagenic risk of avanafil's potential genotoxic impurities†

Yunkai Sun,[ab]* Xiaoxia Wu,[bc] Pei Zuo,[c] Zhao Liu,*[c] Xuepei Miao,[a] Jian Liu[a] and Hairuo Wen*[d]

In the technical route for the synthesis of avanafil, 1-ethyl-(3-dimethylaminopropyl)carbamyldiimide hydrochloride (EDCI) and 1-hydroxybenzotriazole (HOBT) are used as reactive acid–amine binding agents. HOBT contains trace amounts of hydrazine residue, and there is a risk of introducing potentially mutagenic impurities with hydrazide-containing structures. The potentially genotoxic impurities E (**Imp-E**) and F (**Imp-F**) of avanafil with altering hydrazide-structure were synthesized by chemical method; subsequently, the impurities were evaluated and classified according to ICH M7 guidelines. Two complementary quantitative structure–activity relationship (QSAR) evaluation systems (Derek and Sarah) based on expert rules and statistics were used to preliminarily predict the genotoxicity of **Imp-E** and **Imp-F**, and the prediction result of E was suspected to be positive. In the Ames test of **Imp-E** and **Imp-F**, in the dose range of 62.5–1000 μg per plate, with or without the presence of metabolic activation system S9, the number of revertant colonies did not exceed 2 times the number of colonies in the solvent control group and did not show a dose–response relationship, and the test results were negative. **Imp-E** and **Imp-F** were determined to be negative for genotoxicity, which could be controlled as class 5 in ICH M7, that is, non mutagenic impurity.

Received 27th March 2024
Accepted 24th June 2024

DOI: 10.1039/d4ra02345e

rsc.li/rsc-advances

1. Introduction

Avanafil is a novel potent phosphodiesterase-5 (PDE-5) inhibitor (Fig. 1) with rapid onset and few adverse reactions and is used for the treatment of hypertension, hyperlipidemia and hyperglycemia.[1,2] As the fourth-generation drug for the treatment of erectile dysfunction, its safety has been widely concerned. Limit control of drug impurity is an important part of drug quality standard research.[3,4] The process route of drug synthesis involves chemical reagents such as reactants, solvents and catalysts, as well as chemical reactions and degradation. Impurities are unavoidable in raw materials and preparations. In recent years, increasing attention has been paid to the genotoxicity risk of drug impurities, and the European Medicines Agency (EMA) and the US Food and Drug Administration (FDA) have successively promulgated the guiding principles for the control of genotoxic impurities (GTIs).[5,6] In 2014, ICH officially issued the M7 guidelines,[7] which set out general requirements for the control of DNA-active (mutagenic) drug impurities in order to control the evaluation and control of DNA reactive (mutagenic) drug impurities with potential carcinogenic risks and have been used in the drug registration of member states.

Genotoxic impurities refer to DNA reactive substances that could directly cause DNA damage at low levels, leading to DNA mutation and even carcinogenesis.[8,9] Hydrazine has been identified as a mutagenic and carcinogenic compound,[10–15] and the hydrazine group is also an alert structure of typical genotoxic carcinogens in compounds.[16–18] In the synthesis of avanafil, EDCI and HOBT were used as acid–amine condensation agents, while hydrazine was used in the upper source process of HOBT, resulting in residual hydrazine in HOBT.[19] Hydrazine reacts with intermediate 6 (**M6**) to introduce potentially

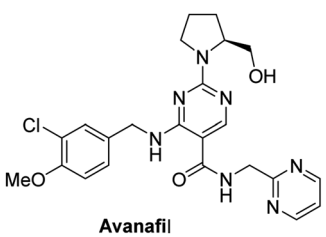

Fig. 1 Structure of avanafil.

[a]School of Chemical Engineering and Materials, Changzhou Institute of Technology, Changzhou 213022, China. E-mail: sunyunkai1983@163.com

[b]School of Chemistry and Chemical Engineering, University of South China, Hengyang 421001, China

[c]Harvest Pharmaceutical Co., Ltd, Changsha 410000, China. E-mail: liuz@harvest-pharm.com

[d]National Center for Safety Evaluation of Drugs, National Institutes for Food and Drug Control, Key Laboratory of Beijing for Nonclinical Safety Evaluation Research of Drugs, Beijing, 100176, P. R. China. E-mail: wenhairuo@nifdc.org.cn

† Electronic supplementary information (ESI) available. See DOI: https://doi.org/10.1039/d4ra02345e

© 2024 The Author(s). Published by the Royal Society of Chemistry

Open Access Article. Published on 08 July 2024. Downloaded on 11/7/2025 2:05:18 AM.
This article is licensed under a Creative Commons Attribution-NonCommercial 3.0 Unported Licence.

mutagenic impurities with warning structures into avanafil. In our synthesis of avanafil, HOBT containing trace hydrazine leads to the creation of impurities (**Imp-E**) with hydrazine groups. Genotoxic impurities have a higher risk of carcinogenesis than common impurities[20,21] and generally have low acceptable limits, posing great challenges to synthesis control processes and detection. Further mutagenic evaluation of the potentially genotoxic impurity of avanafil was performed in accordance with the ICH M7 guidelines: that is, the potential genotoxic impurities E (**Imp-E**) and impurities F (**Imp-F**) are synthesized and confirmed firstly, and then the compound toxicity prediction softwares of Derek Nexus and Sarah Nexus[22–26] were used to predict the risk and possible warning structure of mutation resulting from mutation as the toxicity endpoint. Finally, the bacterial reverse mutation test (Ames test)[27–30] was conducted to provide guidance and a basis for the classification and control of related substances in avanafil.

2. Experimental

2.1 Chemicals and materials

1-Hydroxybenzotriazole (HOBT Guangdong Wengjiang Chemical Reagent Co., LTD.); diethyl ethoxymethylenemalonate and L-prolinol (Qifei Pharmaceutical); *S*-methyl isothiourea semisulfate and 3-chloro-4-methoxybenzylamine hydrochloride (Emeishan Hongsheng Pharmaceutical); *M*-chloroperoxybenzoic acid (Baokang Pharmaceutical Chemical Co., Ltd.); sodium azide (Henan Standard Material Research and Development Center); *O*-benzotriazole-tetramethylurea hexafluorophosphate (HBTU), *N*,*N*-diisopropylethylamine (DIEA), 1-ethyl-(3-dimethylaminopropyl) carbamyldiimide hydrochloride (EDCI), hydrazine sulfate, L-histidine, D-biotin, D-glucose 6-phosphate sodium salt, β-NADP-Na2, ampicillin, tetracycline, crystal purple, mitomycin C, 2-aminoanthracene, 2-aminofluorene, dioxone (Aladdin); agar plate (Bio-high Technology); metabolic activation system S9 (Bioplus Biotech). Citric acid monohydrate, disodium hydrogen phosphate, sodium dihydrogen phosphate, sodium ammonium hydrogen phosphate, D-(+)-glucose, magnesium chloride, potassium chloride, dipotassium phosphate, magnesium sulfate, sodium chloride, anhydrous sodium carbonate, phosphorus oxychloride, methanol, triethylamine (Nanjing Chemical Reagent Co., Ltd.).

2.2 Instruments

Instrument: Bruker Avance III 400 NMR instrument (solvent: DMSO-d_6, internal standard: TMS); high resolution mass spectrometer (UPLC1290/TOF MS 6230); high pressure preparation liquid chromatograph (Bonna-Agela CHEETAH II); ultra-performance liquid chromatography (Agilent 1260 UHPLC system); WTD electronic balance; SGW-3 automatic polarimeter; N-1300 rotary evaporation instrument; SHZ-D vacuum pump; DZF-6051 vacuum drying oven; DHG-9140 electric blast drying oven; SPX-70BE biochemical incubator; NMSP-600 horizontal rotating oscillator; DW-86W28 ultra-low temperature storage box; HYC-3105 medical cooler.

2.3 UPLC and chromatographic conditions

The UPLC method was developed for the analysis of the related impurities on an Agilent 1260 UHPLC system.[31] The chromatographic analysis was carried out on a Waters ACQUITY HSS C18 with 50 mm × 2.1 mm and 1.8 μm particle size column. The mobile phase was composed of 20 mM ammonium formate aqueous solution; pH was adjusted to 5.00 ± 0.05 with dilute formic acid (mobile phase-A) and acetonitrile (mobile phase-B). The gradient program is set to (T_{min}/mobile phase-A : B): T_0/90 : 10, T_1/90 : 10, T_8/20 : 80, T_{10}/90 : 10, T_{11}/10 : 90. It was degassed and filtered through 0.22 μm filters under vacuum before injecting into the system. The mobile phases were set with a flow rate of 0.3 mL min^{-1}, and the column temperature was kept at 35 °C. The analytes were detected in a photodiode array detector at 239 nm.

2.4 High resolution mass spectrometer (HRMS)

HRMS analyses were performed on a UPLC1290/TOF MS 6230 system. Analysis of all compounds was performed on Waters C18 columns. The operating parameters were as follows: a nebulizer gas pressure of 7.5 bar, dry gas flow rate of 5.0 L min^{-1}, capillary voltage of 3.5 kV, ion flight time of 0.5 s, and transfer capillary temperature of 300 °C. All data is collected and processed by Agilent's data analysis software, Mass Hunter.

2.5 Synthesis of target compounds

2.5.1 Synthesis of intermediates M1–6. The synthesis of **M1–6** is referenced in ref. 32, and the route of synthesis is

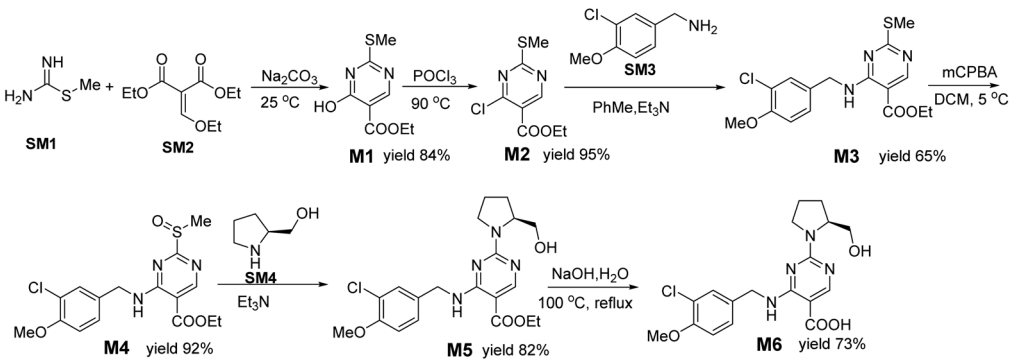

Fig. 2 Synthesis route of intermediate 6 (M6).

Open Access Article. Published on 08 July 2024. Downloaded on 11/7/2025 2:05:18 AM.
This article is licensed under a Creative Commons Attribution-NonCommercial 3.0 Unported Licence.

shown in Fig. 2. Among them, **M5** and 10% NaOH solution were hydrolyzed to obtain **M6**, and the yield was 72.9%, mp 181–182 °C. The NMR spectra and other related data are in agreement with the reported results (see Fig. S3 and S4†).

2.5.2 Synthesis of Imp-E.[31] 2.54 mmol **M6**, 7.62 mmol triethylamine, 3.81 mmol HOBT, 3.81 mmol EDCI were added into a 250 mL single-neck flask with 100 mL dichloromethane and stirred at room temperature for 30 min. After the solution was clarified, 3.82 mmol hydrazine sulfate was added and the reaction continued for 12 hours; then, 5% NaOH solution was added to the reaction solution to remove the incomplete raw materials. The precipitating solid product was filtered, washed with distilled water, purified by ethanol beating, and dried by air at 50 °C to obtain 1.0 g pink solid with a yield of 20%, mp 169.4–170.4 °C (Fig. 3). The relevant physical and chemical data are consistent with the literature reports (see Fig. S1, S5 and S6†). ^{1}HNMR (400 MHz, DMSO-d$_6$) δ: 9.42 (s, 1H), 9.07 (d, J = 11.4 Hz, 1H), 8.32 (s, 1H), 7.39 (s, 1H), 7.28 (dd, J = 8.4 Hz, 2.0 Hz, 1H), 7.08 (s, 1H), 4.92 (s, 1H), 4.67 (s, 1H), 4.52 (d, J = 5.8 Hz, 2H), 4.29 (s, 2H), 4.06 (s, 1H), 3.82 (s, 3H), 3.60 (s, 1H), 3.45 (q, J = 8.2 Hz, 7.0 Hz, 2H), 1.91 (m, 4H); ^{13}C NMR (100 MHz, DMSO-d$_6$) δ: 167.54, 160.88, 160.12, 155.91, 153.81, 133.75, 129.43, 127.94, 113.16, 62.18, 61.52, 59.37, 56.52, 47.53, 42.58, 27.96, 23.29, 23.06.

2.5.3 Synthesis of Imp-F. As shown in Fig. 4, 7.64 mmol **M6**, 11.46 mmol HBTU, 11.46 mmol *N*,*N*-diisopropylethylamine and 10 mL DMF were added to a 50 mL single-neck flask successively. After stirring at 30 °C for 30 min, the solution became clear; at this time, 11.46 mmol hydrazine sulfate was added, and the reaction was carried out overnight (12–14 h). Purified water was added to the reaction solution, precipitating a large amount of solid, which was dried at 50 °C. The solids were purified on a high pressure preparation liquid chromatograph (Bonna-Agela CHEETAH II), using the Ultimate AQ-18 column with mobile phase A as ammonia solution (pH = 7) and mobile phase B as acetonitrile. The gradient program was set to (T_{min}/mobile phase A : B), T_0/70 : 30, T_{70}/60 : 40, T_{200}/50 : 45, the flow rate was 10 mL min^{-1}, and the detection wavelength was maintained at 254 nm. 450 mg of solid was dissolved in about 2 mL solution with DMSO, and the column liquid with **Imp-F** was collected and treated to obtain 65 mg yellow solid with a purity of 95%. mp 161.5–163.3 °C (see Fig. S7 and S8†). ^{1}H NMR (400 MHz, DMSO-d$_6$) δ: 9.95 (s, 2H), 9.00 (s, 2H), 8.50 (s, 2H), 7.40 (s, 2H), 7.28 (d, J = 8.2 Hz, 2H), 7.08 (d, J = 8.4 Hz, 2H), 4.89 (s, 1H), 4.69 (s, 1H), 4.51 (s, 4H), 4.09 (s, 2H), 3.81 (s, 6H), 3.61 (s, 2H), 3.49 (s, 4H), 1.95 (m, 8H), 1.23 (s, 2H); ^{13}C NMR (100 MHz, DMSO-d$_6$) δ: 167.16, 153.89, 133.48, 129.83, 129.59, 128.20, 121.19, 113.15, 59.79, 59.36, 56.52, 47.85, 42.75, 28.01, 22.95.

2.5.4 Specific rotation of Imp-E, Imp-F and intermediates. It can be observed that **M5**, **M6**, **Imp-E** and **Imp-F** have optical activity (Table 1), which originate from L-prolinol (**SM4**) when **M4** is transformed into **M5**. The chiral carbon atom of SM4 is in the *S* configuration. In the process of synthesizing **M5**, **M6**, **Imp-E** and **Imp-F**, the reactive groups do not involve the change of chiral carbon atom configuration. Therefore, it is preliminarily speculated that the chiral carbon atom configuration of **Imp-E** and **Imp-F** are also S-type.

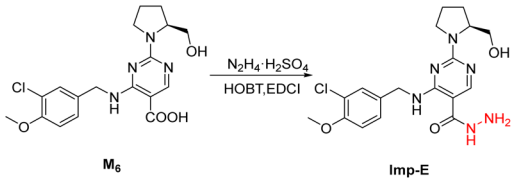

Fig. 3 Synthesis route of Imp-E.

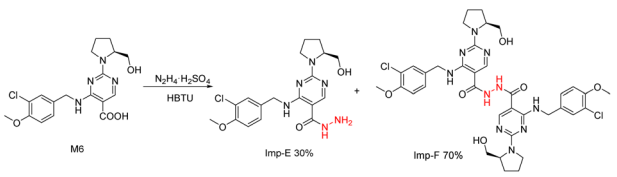

Fig. 4 Synthesis route of Imp-F.

2.6 QASR evaluation model for genotoxicity

Derek Nexus (Derek Nexus version 6.2.1, knowledge base 2022 2.0) provided by Lhasa Limited (Leeds, UK) is a computerized expert system that uses a knowledge-based expert system approach to predict the toxicological hazard of molecules. Thus, it contains expert knowledge rules derived from the known relationship of a given substructure and a toxicological effect of the molecule, and it applies these rules to predict potential toxicological effects of substances for which no experimental data usually exist.

Sarah Nexus (Sarah Nexus version 3.2.0, model 2022.2), provided by Lhasa Limited (Leeds, UK), is a statistics-based system. Structures submitted for processing are fragmented, and these fragments are reviewed for activity *versus* inactivity. The model then arranges those fragments of interest into a network of hypotheses (or nodes) and relevant hypotheses are used to inform an overall prediction of toxicity. Sarah Nexus predicts activity or inactivity in the Ames test and provides information on the coverage of a query compound.

Nexus version: Nexus 2.5.2 is a software integration platform. In this study, the solidified ICH M7 batch classification model in the Nexus system was used to predict and automatically classify the genotoxicity of impurities.

Table 1 Specific rotation of Imp-E, Imp-F and intermediates[a]

Sample	Solvent	Concentration of solution (g per 100 mL)	$[\alpha]_D^t$
SM4	DMF	0.2612	+9.7
M5	DMF	0.2518	−49.5
M6	DMF	0.2534	−92.4
Imp-E	DMF	0.2512	−108.3
Imp-F	DMF	0.2534	−110.5

[a] $[\alpha]_D^t$: t = 20 °C; D = 589 nm.

 © 2024 The Author(s). Published by the Royal Society of Chemistry

Open Access Article. Published on 08 July 2024. Downloaded on 11/7/2025 2:05:18 AM.
This article is licensed under a Creative Commons Attribution-NonCommercial 3.0 Unported Licence.

2.7 Ames test

The test articles were impurities **Imp-E** and **Imp-F**. Positive controls for the Ames test were sodium azide (CAS no. 26628-22-8), mitomycin C (CAS no. 50-07-7), 2-aminofluorene (CAS no. 153-78-6), 2-anthramine (CAS no. 613-13-8) and dioxone (CAS no. 140-56-7), respectively. DMSO, which was used as a solvent for the test chemicals and positive controls, served as the vehicle control.

Salmonella typhimurium histidine-dependent strains TA98, TA100, TA1535, TA102 and TA97a were obtained from Moltox Company. The strains were freeze-dried and stored in the refrigerator at 2–8 °C. The strains were inoculated in nutrient broth medium of 20 mL and cultured at 37 °C (120 times per min) for 11 h. The metabolic activation system (rat liver microsomes, S9) was purchased from IPHASE. S9 mixture (10% S9 v/v) was prepared in a glucose-6-phosphate shortly before use and kept on crushed ice to keep it cold. The top layer medium 2.0 mL containing 0.5 mmol per L histidine and 0.5 mmol per L biotin was divided into a sterilized EP tube and kept warm in a water bath at 50 °C. Then, 0.1 mL of the bacterial suspension, 0.1 mL test substance solution, and 10% (v/v) of liver S9 mixture or phosphate buffer were added. The mixture solution was thoroughly mixed, quickly poured over the surface of an agar plate, and incubated in a 37 °C incubator for 48 h, and the number of reverted colonies per plate was counted. Three parallel plates were made for each dose, and a blank control group, solvent control group and positive control group were set up.

2.8 Statistics

The number of revertant colonies was counted manually, and the average plate counts under each concentration gradient were taken. SPSS 27.0 software was used for statistical analysis of the data. The quantitative statistical description was $\bar{x} \pm s$, and the multiple change of reversed colony number was calculated by comparing with spontaneous control.

3. Results and discussion

3.1 Discovery and structural resolution of Imp-E

The synthesized avanafil samples were analyzed using the newly developed method described in Section 2.3, and the results showed that the **Imp-E** with the retention time (5.836 min) was detected (Fig. 5). The structure of **Imp-E** is determined by mass spectrometry (MS) and nuclear magnetic resonance spectrometry (NMR). The HRMS spectrum (Fig. 6) shows that **Imp-E** has

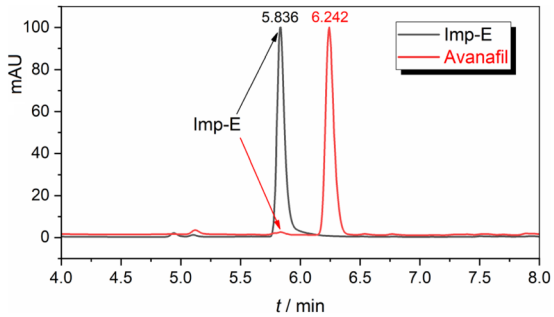

Fig. 5 Liquid chromatogram of avanafil and Imp-E.

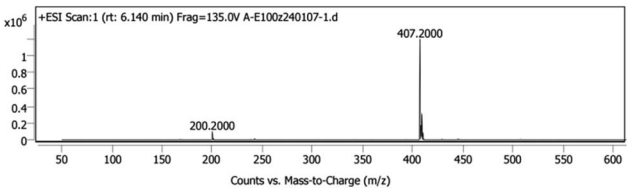

Fig. 6 High resolution mass spectrum of Imp-E.

Table 2 QSAR prediction of Imp-E/Imp-F and the alert structures

		Derek Nexus		Sarah Nexus			
				Reliability			
				Struc. 1	Struc. 2	Struc. 3	
Compd	Structure	Alert structure	Result				Result
Imp-E	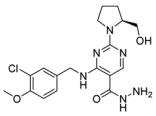		++++ plausible	24%	23%	23%	−□□□ negative
Imp-F	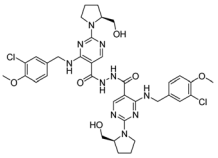		−−−□ inactive	24%	16%	21%	−□□□ negative

Open Access Article. Published on 08 July 2024. Downloaded on 11/7/2025 2:05:18 AM. This article is licensed under a Creative Commons Attribution-NonCommercial 3.0 Unported Licence.

only one high molecular ion peak (*m*/*z* 407.2000). The formation of **Imp-E** is caused by a small amount of hydrazine in HOBT. Although **Imp-F** is not found in avanafil, the confirmation of the structure of **Imp-E** makes us realize that **Imp-F** with mutagenic alert structure needs to be considered as a potential genotoxic impurity.

3.2 QSAR evaluation of Imp-E and Imp-F

Imp-E and **Imp-F** had mutagenic alert structures, and the ICH classification model was used for prediction, as shown in Table 2. Derek Nexus considered that **Imp-E** was suspiciously positive for mutagenic risk due to the presence of hydrazine sulfate, hydrazine hydrate, and isoniazid, which could increase the mutation rate of TA1535. However, for **Imp-F**, the predicted result is inactive. The prediction results of Sarah Nexus were based on the search of compound structure decomposition, and the probability of mutagenic risk between all decomposed structures and substances with the same structure was estimated. Sarah Nexus' prediction results of impurity E and impurity F were negative. The results of computer simulation toxicity assessment of impurity E by QSAR methods based on different principles are inconsistent, and the predicted results between **Imp-E** and **Imp-F** (with a similar structure) are also inconsistent.

Table 3 Genetic identification criteria of *Salmonella typhimurium* (see Fig. S9–S13)

Bacterial strain	His$^-$	Rfa	*R*	pAQ$_1$	UvrB$^-$ repair-deficiency
TA98	+	+	+	−	−
TA97a	+	+	+	−	−
TA100	+	+	+	−	−
TA102	+	+	+	+	+
TA1535	+	+	−	−	−

3.3 Genotype identification of the detected strains

As shown in Table 3, the rfa membrane mutation of the strain increased the permeability of macromolecular compounds, making it easier for macromolecular compounds to enter the bacteria. UvrB-strains have defective excision repair functions and cannot excise DNA adducts, making the strains susceptible to mutagenicity and bacterial toxicity of a large number of mutants. The bacteria containing plasmid pkm101 had a higher number of spontaneous recovery colonies, and plasmid pkm101 had muc+ gene, which was involved in DNA damage-induced DNA repair pathway, and increased the susceptibility to mutability while giving bacteria resistance to bacterial toxicity. The strains with the *R* factor were resistant to ampicillin. Strains containing pAQ1 had tetracycline resistance. The different strains have different sensitivities to mutants. TA98 and TA100 are sensitive to most mutants, and the preliminary screening test can only detect these two strains. In the formal experiment, TA98 and TA97a detected frameshift mutation agents, TA1535 and TA100 detected base-displacement mutagenic agents, and oxidizing mutants, DNA crosslinkers, and hydrazine could be detected by strains TA102 containing AT-site mutations.

3.4 Ames test for Imp-E and Imp-F

Spectral grade DMSO is selected as the solvent to dissolve **Imp-E** and **Imp-F** because it does not react with the subject matter and is not toxic to the strain and S9. Cytotoxicity and the solubility of the substance should be considered when determining the maximum concentration for the Ames test. For compounds with good solubility and no or little cytotoxicity, the maximum dose can be 5 mg per plate.

Preliminary data showed that **Imp-E** and **Imp-F** were toxic in the dose groups of 5000, 2500 and 1600 μg per plate. In the formal test, 1000, 500, 250, 125, 62.5 μg per plate doses were

Table 4 Ames test for Imp-E

		Number of revertants				
Group μg per plate	S9	TA98	TA97a	TA100	TA102	TA1535
1000	−	33 ± 4	129 ± 17	122 ± 11	210 ± 14	41 ± 6
	+	36 ± 4	172 ± 8	159 ± 32	266 ± 12	57 ± 2
500	−	43 ± 5	91 ± 5	124 ± 12	274 ± 8	41 ± 6
	+	37 ± 2	185 ± 9	159 ± 32	241 ± 25	53 ± 3
250	−	41 ± 3	152 ± 34	174 ± 13	223 ± 12	55 ± 2
	+	42 ± 3	178 ± 14	124 ± 13	223 ± 12	54 ± 2
125	−	39 ± 4	144 ± 12	143 ± 15	218 ± 14	61 ± 3
	+	34 ± 3	154 ± 7	158 ± 30	262 ± 7	61 ± 3
62.5	−	34 ± 4	153 ± 19	143 ± 22	264 ± 14	56 ± 2
	+	30 ± 2	194 ± 16	153 ± 25	270 ± 5	57 ± 2
Positive control	−	1111 ± 117[a]	1872 ± 104[a]	1697 ± 54[c]	2043 ± 185[d]	1190 ± 40[c]
	+	1171 ± 78[b]	1920 ± 120[b]	2053 ± 65[b]	2121 ± 21[e]	1323 ± 69[b]
Solvent control	−	27 ± 4	137 ± 24	177 ± 4	196 ± 12	45 ± 5
	+	35 ± 7	164 ± 14	212 ± 31	212 ± 17	47 ± 4
Blank control	−	29 ± 1	152 ± 10	181 ± 15	252 ± 2	50 ± 5
	+	47 ± 4	192 ± 5	183 ± 10	277 ± 4	45 ± 7

[a] Dioxone, 50 μg per plate. [b] 2-Aminofluorene, 20 μg per plate. [c] Sodium azide, 1 μg per plate. [d] Mitomycin C, 1 μg per plate. [e] 2-Aminoanthracene, 20 μg per plate.

 © 2024 The Author(s). Published by the Royal Society of Chemistry

Open Access Article. Published on 08 July 2024. Downloaded on 11/7/2025 2:05:18 AM.
This article is licensed under a Creative Commons Attribution-NonCommercial 3.0 Unported Licence.

Table 5 Ames test for Imp-F

		Number of revertants				
Group μg per plate	S9	TA98	TA97a	TA100	TA102	TA1535
1000	−	16 ± 3	57 ± 6	174 ± 12	201 ± 7	41 ± 2
	+	31 ± 5	38 ± 7	184 ± 12	172 ± 22	33 ± 2
500	−	26 ± 4	129 ± 26	131 ± 11	235 ± 13	38 ± 4
	+	30 ± 3	137 ± 12	181 ± 10	208 ± 11	35 ± 7
250	−	34 ± 3	107 ± 13	167 ± 19	262 ± 8	25 ± 4
	+	38 ± 2	161 ± 31	189 ± 2	226 ± 14	23 ± 2
125	−	28 ± 9	98 ± 5	169 ± 5	257 ± 15	37 ± 2
	+	28 ± 8	146 ± 32	192 ± 9	209 ± 22	35 ± 5
62.5	−	31 ± 6	142 ± 6	151 ± 15	274 ± 6	33 ± 2
	+	36 ± 2	177 ± 9	184 ± 7	273 ± 2	32 ± 2
Positive control	−	1111 ± 117[a]	1872 ± 104[a]	1697 ± 54[c]	2043 ± 185[d]	1333 ± 53[c]
	+	1171 ± 78[b]	1920 ± 120[b]	2053 ± 65[b]	2121 ± 21[e]	1534 ± 77[b]
Solvent control	−	32 ± 1	137 ± 24	177 ± 4	242 ± 10	43 ± 5
	+	35 ± 4	164 ± 14	212 ± 31	227 ± 10	47 ± 3
Blank control	−	29 ± 1	152 ± 10	181 ± 15	252 ± 2	38 ± 1
	+	47 ± 4	192 ± 5	183 ± 10	277 ± 4	48 ± 4

[a] Dioxone, 50 μg per plate. [b] 2-Aminofluorene, 20 μg per plate. [c] Sodium azide, 1 μg per plate. [d] Mitomycin C, 1 μg per plate. [e] 2-Aminoanthracene, 20 μg per plate.

applied. As shown in Tables 4 and 5, the number of revertants in the solvent control group was within the normal range, and the number of revertants in the different positive control groups was more than 2 times that of the solvent control group. **Imp-E** and **Imp-F** at the dose of 1000, 500, 250, 125, 62.5 μg per plate had no difference in the number of revertants induced by TA97a, TA98, TA100, TA102 and TA1535 compared with the solvent control group and showed a dose-independent effect. There was also no reproducible positive response for a single test point. These results suggested that hydrazine with large steric acyl substitution reduces the genotoxicity of hydrazine, and that hydrazine compounds containing 1 or 2 acyl substitutions have no mutagenic effect and cannot cause base substitution and shift-type mutation. **Imp-F** showed a similar result. These indicated that both **Imp-E** and **Imp-F** were not mutagenic to *Salmonella typhimurium*.

4. Conclusions

In this study, the potential mutagenic impurities **Imp-E** and **Imp-F** of avanafil were synthesized using the design method. QSAR genotoxicity assessment and Ames test were performed for **Imp-E** and **Imp-F** according to ICH M7 requirements. The QSAR evaluation showed that Derek's prediction of **Imp-E** was positive and that of **Imp-F** was inactive. Sarah's prediction results for **Imp-E** and **Imp-F** were negative, and the prediction results could not accurately distinguish the toxicity differences of compounds having structural differences. The results of the Ames test showed that the genotoxicity of **Imp-E** and **Imp-F** in 62.5–1000 μg per plate was negative with or without the presence of S9. In summary, the results eliminate concerns about the genotoxicity of **Imp-E** and **Imp-F** based on the altered structure of the hydrazine group. **Imp-E** and **Imp-F** could be classified as class 5 impurities, that is, ordinary impurities. This study provides theoretical guidance and an experimental basis for the classification and classification control of potential genotoxic impurities **Imp-E** and **Imp-F** in avanafil.

Data availability

All relevant data are included in the manuscript, along with additional information.

Author contributions

Yunkai Sun: writing-original draft, supervision, funding acquisition; Xiaoxia Wu: investigation, experiment, data curation; Pei Zuo: design of Ames test; Zhao Liu: experimental design, supervision and revise the paper; Xuepei Miao: instruction of the experiment; Jian Liu: revise the paper. Hairuo Wen: QSAR evaluation, revise the paper. All authors read and approved the final manuscript.

Conflicts of interest

There are no conflicts to declare.

Acknowledgements

This work was supported by the Natural Science Foundation of Hunan Province (No. 2022JJ80096), Natural Science Foundation of the Jiangsu Higher Education Institutions of China (23KJA150003) and Fund of CIT (YN22039).

Notes and references

1 M. Kumar, A. D. Pathade, V. B. Gupta, S. V. Gupta, S. Goyal, D. Rath, M. Thakre, J. Sanmukhani and R. Mittal, *Int. J. Urol.*, 2022, **29**(4), 351–359.

Open Access Article. Published on 08 July 2024. Downloaded on 11/7/2025 2:05:18 AM.
This article is licensed under a Creative Commons Attribution-NonCommercial 3.0 Unported Licence.

2 J. Li, L. Peng, D. Cao, L. J. He, Y. X. Li and Q. Wei, *J. Mens Health*, 2019, **13**(5), 1557–9883.
3 R. K. Chawla, S. Panda, K. Umasankar, S. P. Panda and D. Damayanthi, *Curr. Pharm. Anal.*, 2020, **16**(7), 801–805.
4 D. Pokar, N. Rajput and P. Sengupta, *Int. J. Pharm.*, 2020, **576**, 119018.
5 D. K. Singh, A. Sahu, S. Kumar and S. Singh, *TrAC, Trends Anal. Chem.*, 2018, **101**, 85–107.
6 R. Holm and D. P. Elder, *Eur. J. Pharm. Sci.*, 2015, **87**, 118–135.
7 European Medcines Agency (EMA), *Guideline on the Limits of Genotoxic Impurities [EB/OL] (2006-06-28) [2020-02-22]*, **https://www.ema.europa.eu/en/documents/scientific-guideline/guideline-limits-genotoxic-impurities_en.pdf**.
8 European Medcines Agency (EMA), *Questions & answers on the CHMP Guideline on the Limits of Genotoxic Impurities [EB/OL] (2010-09-23) [2020-02-22]*, **https://www.ema.europa.eu/en/documents/scientific-guideline/questions-answers-guideline-limits-genotoxic-impurities_en.Pdf**.
9 *International Conference on Harmonisation (ICH) M7 (R2), Assessment and Control of DNA Reactive (Mutagenic) Impurities in Pharmaceuticals to Limit Potential Carcinogenic Risk Impurities [EB/OL]*, (2023-07), **https://www.fda.gov/media/170461/download**.
10 M. E. Crosby, R. Ciurlionis, T. G. Brayman, A. Kondratiuk and J. J. Nicolette, *Environ. Mol. Mutagen.*, 2022, **63**(7), 336–350.
11 IARC Working Group on the Evaluation of Carcinogenic Risks to Humans, *Some Industrial Chemicals*, International Agency for Research on Cancer, Lyon (FR), 2018, PMID: 29863829.
12 B. Z. Levi, J. C. Kuhn and S. Ulitzur, *Mutat. Res. Lett.*, 1986, **173**(4), 233–237.
13 J. Nicolette, J. Murray, P. Sonders, J. Murray, P. Sonders, A. Kondratiuk and M. Crosby, *Environ. Mol. Mutagen.*, 2021, **62**(1), 4–17.
14 L. Malcamor and A. A. Stark, *Appl. Environ. Microbiol.*, 1982, **44**(4), 801–808.
15 A. V. Wright and L. Tikkanen, *Mutat. Res., Fundam. Mol. Mech. Mutagen.*, 1980, **78**(1), 17–23.
16 T. Maeda, A. Shibai, N. Yokoi, Y. Tarusawa, M. Kawada, H. Kotani and C. Furusawa, *Mutat. Res., Fundam. Mol. Mech. Mutagen.*, 2021, **823**, 111–759.
17 P. Silvio, T. Maurizio, R. Patrizia, P. Mauro, T. Marisa and M. B. Carlo, *Carcinogenesis*, 1981, **2**(12), 1317–1326.
18 S. A. Glover, *Aust. J. Chem.*, 2023, **76**(1), 1–24.
19 D. S. Treitler, A. S. Marriott, J. Chadwick and E. Quirk, *Org. Process Res. Dev.*, 2019, **23**(11), 2562–2566.
20 M. A. Sandhu, A. A. Saeed, M. S. Khilji, A. L. Anwaar, S. Z. Malik and N. Khalid, *J. Toxicol. Sci.*, 2013, **38**(2), 237–244.
21 G. Susanne, O. Ulrich, E. Azeddine, S. Muthusamy, R. Sangana, H. J. Martus, T. Bedman and A. Hartmann, *Regul. Toxicol. Pharmacol.*, 2022, **134**, 105245.
22 J. Yin, H. Wen and H. Chen, *J. Appl. Toxicol.*, 2023, **43**(2), 230–241.
23 A. B. Raies and V. B. Bajic, *Wiley Interdiscip. Rev.: Comput. Mol. Sci.*, 2016, **6**(2), 147–172.
24 M. Honma, A. Kitazawa, T. Kasamatsu and K. I. Sugiyama, *Gene Environ.*, 2020, **42**(1), 32–37.
25 T. Kasamatsu, A. Kitazawa and S. Tajima, *Gene Environ.*, 2021, **43**(1), 1–17.
26 A. Sutter, A. Amberg, S. Boyet, F. J. Contrera, L. L. Custer and L. K. Dobo, *Regul. Toxicol. Pharmacol.*, 2013, **67**(1), 39–52.
27 M. S. Diehl, S. L. Willaby and R. D. Snyder, *Environ. Mol. Mutagen.*, 2015, **36**(1), 72–77.
28 M. O. Kenyon, J. R. Cheung, K. L. Dobo and W. K. Warren, *Regul. Toxicol. Pharmacol.*, 2007, **48**(1), 75–86.
29 K. P. Cross and D. M. DeMarini, *Mutat. Res.*, 2023, **827**, 111838.
30 B. C. Fischer, Y. Musengi, J. Konig, B. Sachse, S. Hessel-Pras, B. Schafer, C. Kneuer and K. Herrmann, *Mutagenesis*, 2024, **39**(1), 32–42.
31 Y. K. Sun, X. X. Wu, M. Cao, X. Q. Xue, D. f. Jiang and Z. Liu, *J. Mol. Struct.*, 2024, **1295**, 136601.
32 Y. Koichiro, M. Kenji and O. Kenii, *et al.*, *US Pat.*, US20030229095A1, 2003.

 © 2024 The Author(s). Published by the Royal Society of Chemistry